SEVENTH SYMPOSIUM
TURBULENT SHEAR FLOWS
Stanford University
August 21-23, 1989

Grid-Independent Wall Layer Turbulence Model for Complex Flow Calculations

Mark J. Jennings
Illinois Institue of Technology, Chicago, Illinois

Thomas Morel
Ricardo-ITI, Westmont, Illinois

ABSTRACT

A new modeling approach has been developed for the near wall region in turbulent flows, to be used as an alternative to wall functions in multi-dimensioinal flow simulation codes. The model involves the solution of a set of boundary layer equations on a finely resolved one-dimensional grid spanning the wall layer (below y^+=50). The wall layer grid is dynamically scaled to provide sufficient resolution of the near wall flow regardless of the resolution of the bulk flow grid. The wall layer solution does not rely on the assumption of turbulence equilibrium (production=dissipation), making it applicable to complex flows involving separation and reattachment. Comparison to skin friction and heat transfer data in sudden expansion flows shows that the new model performs significantly better than the wall functions.

INTRODUCTION

The ability of multi-dimensional flow simulation codes to accurately calculate skin friction and convective heat transfer in complex turbulent flows is an important factor in determining the usefulness of these codes as design analysis tools. Most multi-dimensional codes currently being used for engineering calculations employ simple turbulence models that have been developed and tested in the context of two-dimensional boundary layers. There exists a real need for enhancements to these models which would allow them to be applied to practical flow configurations with a sufficient level of confidence.

In this paper, a new treatment of the near wall flow is presented that is more general and flexible than conventional wall turbulence models and, as a result, is better suited for complex flow calculations. The methodology will be described in the context of a standard two equation k-ϵ model, however, the basic approach can be readily extended to higher order turbulence closures.

WALL FUNCTION APPROACH TO NEAR WALL MODELING

The approach to handling the near wall flow that has gained the most widespread acceptance makes use of wall functions. The wall function relations determine the wall shear stress and heat flux as functions of the flow field variables at the near wall nodes. In addition, they determine near wall levels of turbulence production and dissipation. These quantities are then applied as boundary conditions on the outer flow equations at the near wall nodes.

The most common approach to deriving the wall function relations for the mean flow variables is based on the assumption of a two zone (inner viscous zone, outer turbulent zone) wall layer flow (Launder and Spalding, 1972), across which the shear stress and heat flux are constant. As a result, mean profiles of streamwise velocity and temperature have a linear shape in the fully viscous zone and a logarithmic shape in the fully turbulent zone. The near wall turbulence field is assumed to be in equilibrium (energy production=energy dissipation), resulting in explicit expressions for the near wall turbulence production and dissipation. The equations associated with the two zone wall layer model as described are summarized in Table I. While there have been more sophisticated wall function relations developed over the years (e. g. see Patankar and Spalding (1967), Patel (1972), Viegas et al (1985), Chieng and Launder (1980), and Amano (1984)), most treatments are based on a two zone analysis. As a result, the form presented in Table I can be considered representative of wall function treatments currently being used.

For complex flow calculations, the wall function treatment of the wall layer flow suffers from numerous deficiencies including:

- Predictions of wall shear stress are sensitive to the location of the solution grid point nearest to the wall. This is magnified by the discontinuous treatment of the turbulent transport within the wall layer flow applied in the derivation of the wall functions.

- The wall functions are based on assumptions which are only strictly valid in simple boundary layer flows. In particular, the assumption of turbulence equilibrium is severely violated in flow regions near separation and reattachment.

- The wall function conditions are only applied at the node nearest the wall. Depending on local flow conditions and the location of grid points, several nodes beyond the near wall node can lie within the wall layer. As a result, the bulk flow turbulence equations are solved in a region where they are not valid.

Table I. Wall Function Equations.

Near wall parameters:

$y^+ = \rho u_* y/\mu$
$W^+ = W/u_*$
$T^+ = \rho u_* (h_w - h)/q_w$
$u_* = C_\mu^{1/4} \sqrt{k}$
y = normal distance to wall
W = tangential mean velocity at y
h_w = mean fluid enthalpy at the wall
h = mean fluid enthalpy at y
k = turbulent kinetic energy at y
ρ = fluid density
q_w = wall heat flux
C_μ = 0.09

Mean velocity:

$W^+ = y^+ \qquad y^+ \le 11.63$
$W^+ = \ln(Ey^+)/\kappa \qquad y^+ > 11.63$
$E = 9.793 \qquad \kappa = 0.4187$

Mean fluid enthalpy:

$T^+ = \sigma_h y^+ \qquad y^+ \le 11.63$
$T^+ = \sigma_{h,t}[\ln(Ey^+)/\kappa + P(\sigma_h/\sigma_{h,t})] \qquad y^+ > 11.63$
$P(\sigma_h/\sigma_{h,t}) = 9(\sigma_h/\sigma_{h,t} - 1)(\sigma_h/\sigma_{h,t})^{-0.25}$

σ_h = molecular Prandtl number
$\sigma_{h,t}$ = turbulent Prandtl number = 1.0

Turbulent kinetic energy:

$P_k = |\tau_w W|/y$
P_k = production of turbulent kinetic energy
τ_w = wall shear stress

Turbulent energy dissipation rate:

$\epsilon = C_\mu^{3/4} k^{3/2}/(\kappa y)$

BOUNDARY LAYER APPROACH TO NEAR WALL MODELING

An alternative approach to modeling the wall layer flow has been developed here in order to overcome the limitations of conventional wall function treatments and provide a physically better representation for complex flows. In this approach, the flow is divided into an outer region consisting of the bulk of the flow, which is solved on a global grid, and a very thin boundary layer region, adjacent to solid boundaries, which is solved on a separate grid. The flow in the boundary layer region is determined by solving a set of boundary layer equations on finely resolved one-dimensional grids that connect the bulk flow grid lines with the walls bounding the flow. The boundary layer grids are locally scaled to span a specified y^+ domain which begins in the viscous sublayer and extends into the fully turbulent region (beyond $y^+ = 50$) of the wall layer. As a result, the dimensional distances normal to the wall over which the grids extend vary with position in the flow. The boundary layer solution is coupled to the bulk flow solution through matching conditions to ensure a smooth transition between them.

The equations for the boundary layer wall model valid for two-dimensional and axisymmetric flow calculations are presented in Table II. These equations govern the mean velocity parallel to the wall, the turbulent kinetic energy and the mean thermal energy. The equations are derived from their fully-elliptic bulk flow form by using the standard boundary layer assumptions. The wall shear stress and heat flux are calculated directly from derivatives of the mean velocity and temperature, respectively, at the boundary layer grid point closest to the wall. These values are then applied as boundary conditions on the bulk flow grid. The boundary layer k and ϵ solutions overwrite the bulk flow solution at grid points that overlap the wall layer grid.

The turbulent length scale in the boundary layer region receives special treatment in order to provide an accurate representation of the wall layer turbulence. For the region below $y^+ = 50$, a prescribed length scale profile based on a van Driest damping function is used, while in the region beyond $y^+ = 50$ out to the edge of the wall layer grid, a boundary layer form of the dissipation equation is solved. The slope of the prescribed length scale profile at $y^+ = 50$ is matched with the k-ϵ solution in order to ensure a smooth length scale variation from the outer flow all the way down to the wall. Solving the dissipation equation on the boundary layer grid beyond $y^+ = 50$ allows accurate determination of the length scale slope and makes the calculation of the slope independent of the outer flow grid point locations.

The y^+ coordinates at a given position along the wall are calculated from a local value of the wall layer velocity scale, u_*, that depends on the near wall turbulence level (see Table II). The constant C_u in this relation is a weak function of the turbulence Reynolds number in the wall layer and has been tuned to reproduce the friction velocity, $u_\tau = \sqrt{\tau_w/\rho}$, for simple boundary layers and fully developed duct flows. The grid points of the boundary layer mesh are located so that a fixed number of points always resides in the region below $y^+ = 50$. This ensures that the viscous sublayer and buffer layer regions of the wall layer are always adequately resolved.

The important features and potential benefits of the model can be summarized by the following:

The method of calculating the wall layer flow fully coupled with the outer flow reduces the reliance on prescribed near wall flow behavior that is inherent in wall function approaches.

The dynamic positioning of the local boundary layer grids according to a specified y^+ domain means that a priori knowledge of the wall layer thickness is not required when setting up the outer flow grid and the wall model calculations of wall shear stress and heat flux are decoupled from the near wall resolution of the outer grid.

Use of a prescribed length scale profile eliminates the need to solve the dissipation equation very close to the wall where it is most inaccurate. Adjusting the slope according to the local k-ϵ solution makes the profile responsive to outer flow conditions.

The pressure field is solved only on the outer flow grid. Its variation is imposed on the wall layer grid which allows for a relatively inexpensive solution of the wall model equations.

The concept of dividing the flow into bulk and near wall regions has been applied by others to the calculation of complex turbulent flows (Launder, 1988; Iacovides et al, 1987; Chen and Patel, 1988). The basic objective is the same, which is to resolve the near wall region better and apply a different turbulence model to the wall layer flow. The present formulation has several unique features which significantly distinguish it from prior work. The most notable is the dynamic scaling of the wall layer grid. In addition, the use of one-dimensional grid lines in conjunction with the simplified set of boundary layer equations in the wall layer is an approach that has not been taken before. Another unique feature is the length scale formulation in which the prescribed length scale responds to outer flow conditions.

DISCUSSION OF RESULTS

The boundary layer model has been tested and compared to the wall function model and experimental data in a variety of flow configurations including developing and fully developed pipe flow, fully developed channel flow, backward facing step channel flow and sudden expansion pipe flow. In all of these cases the boundary layer model performance either matched or surpassed that of the wall functions. In the discussion to follow some of the results of the channel and pipe sudden expansion flow calculations will be described. For these calculations, the bulk flow equations governing unsteady, incompressible flow in two-dimensional and axisymmetric geometries with heat transfer were solved using a multi-dimensional flow code developed by Dr. A. D. Gosman of Imperial College, London. The standard k-ϵ model as given in Launder and Spalding (1972) was used to model the bulk flow turbulence.

For the sudden expansion flows considered, the channel flow had a step in one wall and was two-dimensional, while the pipe flow had a step change in diameter and was axisymmetric. These are cases, in which complex flow conditions exist, that are well suited for examining the behavior of the near wall models.

During the course of conducting the channel flow calculations it became apparent that the length of the recirculation zone was consistently being underpredicted by approximately 20% of the value indicated by wall shear stress measurements. It was also found, not surprisingly, that the location of the flow reattachment point was almost exclusively determined by the bulk flow solution. The discrepancy in reattachment length made testing of the near wall models and comparisons to data difficult. Therefore, it was decided that the bulk flow model should be slightly modified with the sole purpose of making the channel flow test cases more suitable for investigating the near wall model performance. In order to reduce the spreading rate of the separated shear layer, the C_1 constant appearing in the bulk flow dissipation equation was allowed to vary from its base value. C_1 was made a function of the local turbulence energy production in

Table II. Boundary Layer Wall Model Equations.

Momentum, energy and turbulence energy equations:

$$\rho W W_{,z} + \rho U W_{,y} = -P_{,z} + (\mu_e W_{,y})_{,y}$$

$$\rho W T_{,z} + \rho U T_{,y} = ((\mu/\sigma_h + \mu_t/\sigma_{h,t})T_{,y})_{,y}$$

$$\rho W k_{,z} + \rho U k_{,y} = (((\mu+\mu_t)/\sigma_k)k_{,y})_{,y} + P_k - \rho\epsilon$$

Turbulence dissipation equation (only for $y^+ > 50$) :

$$\rho W \epsilon_{,z} + \rho U \epsilon_{,y} = (((\mu+\mu_t)/\sigma_\epsilon)\epsilon_{,y})_{,y} + C_1(\epsilon/k)P_k - \rho C_2 \epsilon^2/k$$

Matching conditions with outer flow ($y = y_o$):

$$W = W_o \qquad T = T_o \qquad k = k_o \qquad \epsilon = \epsilon_o$$

Length scale matching conditions at y^+=50 :

$$\ell_i = \ell_{50} \qquad (\ell_i)_{,y} = (\ell_{50})_{,y}$$

Additional relations:

$$\mu_t = \rho C_\mu^{1/4} \sqrt{k}\, \ell$$

$$\epsilon = C_\mu^{3/4} k^{3/2}/\ell \text{ for } y^+ \le 50$$

$$\ell_i = \kappa y(1-\exp(-y^+/A^+))$$

κ = $\kappa(y)$, given by length scale matching conditions

$y^+ = \rho u_* y/\mu$

$u_* = C_u k_{max}^{1/2}$

k_{max} = maximum k below y^+=50

C_u = function of $\rho\, k_{max}^{1/2}\, y_{max}/\mu$

y_{max} = y at k_{max}

$C_\mu = 0.09 \quad \sigma_k = 1.0 \quad \sigma_{h,t} = 1.0$

$\sigma_\epsilon = 1.22 \quad C_1 = 1.44 \quad C_2 = 1.92 \quad A^+ = 26.0$

$U = U_o(y/y_o)^2 \qquad P_{,z} = (P_{,z})_o$

Nomenclature:

- W - mean velocity parallel to wall
- U - mean velocity normal to wall
- P - mean pressure
- T - mean temperature
- k - turbulent kinetic energy
- y - coordinate direction normal to wall
- z - coordinate direction parallel to wall
- P_k - turbulence energy production
- μ - fluid molecular viscosity
- ρ - fluid density
- σ_h - molecular Prandtl number
- Subscript o denotes conditions at the first outer flow grid point located beyond $y^+ = 50$.
- Subscript i denotes conditions below y^+=50.
- Subscript 50 denotes conditions determined by the k-ϵ solution at y^+=50.
- Subscript ,y denotes partial derivative with respect to y.
- Subscript ,z denotes partial derivative with respect to z.

the bulk flow away from the solid boundaries. The nature of the function was such that C_1 was increased in a highly localized manner within the narrow central portion of the separated shear layer where the turbulence intensity is the highest. Throughout the remainder of the flow it retained its baseline value. For the channel flow cases to be discussed C_1 was increased by a maximum of 10%. The agreement seen in the predictions of reattachment length for these flows should be understood to have been produced solely by the adjustment of C_1. C_1 was left unchanged for all of the sudden expansion pipe flow cases because the experimental data set used for comparisons did not include measurements of reattachment lengths.

For all of the calculations, ten node points were used in the boundary layer grid below y^+=50. Between y^+=50 and the outer flow match point there were up to ten additional points. As a result, the total number of boundary layer grid points at any location within the flow never exceeded twenty. The overhead associated with the boundary layer model in comparison to the wall function model was not excessive. It is estimated that, when fully optimized, the computation time for the boundary layer solution will be about 20% greater than that for the wall functions on the bulk flow solution grids used here. The wall model overhead is reduced even further as the bulk flow grid is refined.

Wall Shear Stress Results. Two backward facing step channel flows are considered corresponding to the experimental setups of Adams et al (1984) and Westphal et al (1980). The features of each configuration are summarized in Table III along with details of the meshes used for the calculations. For both cases, the inlet conditions at the top of the step were fully turbulent with boundary layer thicknesses given in the table.

Calculated near wall profiles of turbulent kinetic energy and turbulent length scale at one streamwise position near reattachment are shown in Figure 1 for the Adams case. The boundary layer wall model k levels are quite high near the wall in response to turbulent diffusion from the outer flow. By comparison, the k levels calculated with the wall functions are too low, indicating a lack of response to outer flow conditions. The turbulent length scale profile shows that the length scale of the boundary layer model responds to the near wall presence of large scales in the outer flow. On the other hand, for the wall function results, the length scale at the near wall node is fixed by the location of the node which results in the physically implausible break in the length scale profile slope shown in Figure 1. This break appears at all streamwise locations.

The differences in the predicted wall layer turbulence behavior result in significant differences in skin friction predictions (Figure 2). For both the Adams case, Figure 2a, and the Westphal case, Figure 2b, the boundary layer wall model shows good agreement with the data in the region near reattachment and beyond. The peak level of shear stress in the recirculation zone and the shear stress levels near the step face are overpredicted. The wall function predictions are consistently below the measured skin friction along the entire wall beginning near the center of the recirculation zone.

The impact of outer flow turbulence conditions on the near wall flow can be appreciated by considering the boundary layer model turbulent energy budget as a function of streamwise position at the location y^+=50 for the Adams backward facing step flow case (Figure 3). As can be seen from the figure, turbulent diffusion from the outer flow is balanced by turbulent dissipation in the wall layer throughout the recirculation zone, while turbulence production is essentially negligible. Turbulence generated in the separated shear layer is transported to the wall where it is dissipated. This is in sharp contrast to simple boundary layer flows where turbulence production balances dissipation at the wall.

The wall function skin friction predictions shown in Figure 2 are for one particular location of the near wall node points. Significant changes in these predictions occur when the near wall node position is changed as seen in Figure 4. This figure shows shear stress predictions for the Westphal case generated using different bulk flow grids. The total number of node points for each grid is the same while the position of the node points adjacent to the lower wall have been varied. It can be seen from this figure that the wall function results change significantly with the near wall node position particularly when they are positioned below the viscous zone cutoff along the entire lower wall. The boundary layer model predictions are insensitive to this grid parameter, as the figure shows.

Heat Transfer Results. Calculations of three cases of sudden expansion pipe flow are summarized in Table III. The cases considered had a constant wall heat flux imposed downstream of the expansion and represented cases measured in the experimental study of Baughn, et al (1984). The predicted values of Nusselt number are shown in Figure 5 for all of the cases. The Nusselt numbers have been normalized by their fully developed values downstream of the expansion as calculated from the Dittus-Boelter correlation given in Baughn, et al (1984). As can be seen from the figure, the normalized values are larger than one, indicating that the heat transfer from the pipe wall is enhanced by the presence of the reattaching flow. The boundary layer model shows good agreement with the data for all cases in the region beyond the peak Nusselt number location (which is the region beyond flow reattachment). In the recirculation zone, particularly near the step face, the model tends to overpredict the heat transfer coefficient. The wall functions consistently underpredict the level of heat transfer enhancement.

The heat transfer calculations were repeated for one of the cases (expansion ratio = 1.88 and Reynolds number = 68000) using different near wall grid point locations as was done with the backward facing step flow (Figure 4). The purpose was to illustrate the sensitivity of the wall model heat transfer predictions to this grid parameter. Figure 6 shows the resulting Nusselt number predictions for each grid. As was the case with the shear stress predictions in the channel flow, the wall function Nusselt number predictions are very sensitive to the near wall node position while the boundary layer model heat transfer predictions are not.

Table III. Summary of Flow Configurations.

Backward Facing Step Channel Flow:

Case	ER	Re	Inlet δ/h	Grid
Adams (1984)	1.25	36000	1.0	35 x 60
Westphal (1980)	1.67	37000	0.4	35 x 60

ER = channel outlet height/inlet height
$Re_h = \rho W_{ref} h/\mu$ W_{ref} = max inlet velocity
δ = boundary layer thickness h = step height

Sudden expansion Pipe Flow:

Case	ER	Re	Grid (r x z)
1	1.88	68000	35 x 60
2	1.25	39000	35 x 60
3	3.76	17000	35 x 60

ER = outlet pipe diameter/inlet pipe diameter
Re = $\rho WD/\mu$ W = outlet average velocity
D = outlet pipe diameter
All data was taken from Baughn et al (1984).

CONCLUSIONS

A new boundary layer wall model has been developed as an alternative to wall function treatments of the wall layer flow. From comparison of the model predictions with the conventional two zone wall function predictions and experimental data the following conclusions can be drawn:

Wall Function Model -

Limited response is shown to outer flow turbulence conditions even in regions of high turbulent transport from the outer flow. This is partly due to the prescription of a length scale that depends only on the distance from a wall.

Predictions of wall shear stress and heat transfer are highly sensitive to the location of the near wall grid points, particularly when the near wall node crosses the viscous/turbulent zone interface.

Skin friction coefficient and Nusselt number are severely underpredicted compared to measurements for different expansion ratios and Reynolds numbers.

Boundary Layer Wall Model -

A physically realistic response is shown to high levels of turbulent transport from the bulk flow.

The model predictions of shear stress and heat transfer are independent of the near wall resolution of the bulk flow grid. This makes the model particularly attractive for complex flow calculations where a priori knowledge of the wall layer thickness is not available.

The model predictions of skin friction and Nusselt number show an overall level of good agreement with experimental data for different Reynolds numbers and expansion ratios in both two-dimensional and axisymmetric flows. Agreement is particularly good beyond reattachment.

ACKNOWLEDGEMENT

This work was supported by contract DE-AC04-86AL33183 from the Department of Energy's Energy Conversion Technology Program managed by Mr. M. Gunn, under the technical direction of Dr. W. J. McLean at Sandia National Laboratories. The authors acknowledge advice provided by Dr. A. D. Gosman of Imperial College, London on the use of the flow code.

REFERENCES

1. Adams, E. W., Johnston, J. P. and Eaton, J. K., 1984, 'Experiments on the Structure of Turbulent Reattaching Flow', Thermo. Rep. MD-43, Stanford.
2. Amano, R. S., 1984, 'Development of a Turbulence Near-Wall Model and Its Application to Separated and Reattached Flows', Num. Heat Tran., Vol. 7.
3. Baughn, J. W., Hoffman, M. A., Takahashi, R. K. and Launder, B. E., 1984, 'Local Heat Transfer Downstream of an Abrupt Expansion in a Circular Channel with Constant Wall Heat Flux', ASME Jnl of Heat Trans., Vol. 106.
4. Chen, H. C. and Patel, V. C., 1988, 'Near-Wall Turbulence Models for Complex Flows Including Separation', AIAA Jnl, Vol. 26, No. 6.
5. Chieng, C. C. and Launder, B. E., 1980, 'On the Calculation of Turbulent Heat Transport Downstream from an Abrupt Pipe Expansion', Num. Heat Tran., V 3.
6. Iacovides, H., Launder, B. E. and Loizou, P. A., 1987, 'Numerical Computation of Turbulent Flow Through a Square-Sectioned 90 Degree Bend', Int. Jnl. of Heat and Fluid Flow, Vol. 8, No. 4.
7. Launder, B. E. and Spalding, D. B., 1972, Lectures in Mathematical Models of Turbulence, Academic Press.
8. Launder, B. E., 1988, 'On the Computation of Convective Heat Transfer in Complex Turbulent Flows', ASME Jnl of Heat Tran., Vol. 110.
9. Patankar, S. V. and Spalding, D. B., 1967, Heat and Mass Transfer in Boundary Layers, CRC Press.
10. Patel, V. C., 1972, 'A Unified View of the Law of the Wall Using Mixing Length Theory', Aero. Quart., Vol. 24.
11. Viegas, J. R., Rubesin, M. W., and Horstman, C. C., 1985, 'On the Use of Wall Functions as Boundary Conditions for Two-Dimensional Separated Compressible Flows', AIAA Pap. AIAA-85-0180.
12. Westphal, R. V., Eaton, J. K. and Johnston, J. P., 1980, 'A New Probe for Measurement of Velocity and Wall Shear Stress in Unsteady, Reversing Flows', ASME Winter Annual Meeting, November 16-21.

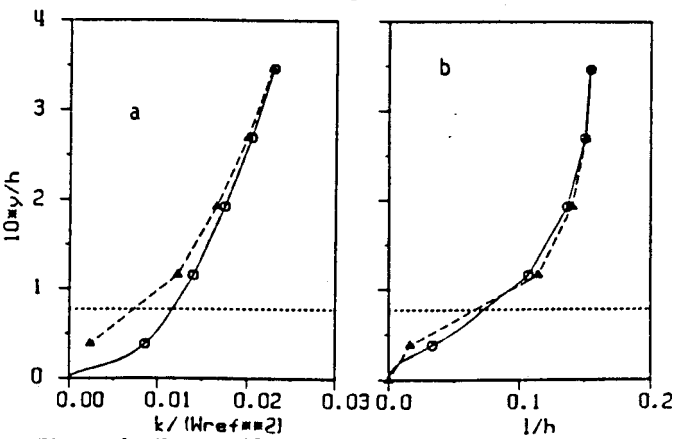

Figure 1. Near wall turbulent energy, (a), and length scale, (b), near reattachment for the Adams channel flow case. Solid line - BL model; Dashed line - wall functions; Symbols - bulk flow grid points; Dotted line - BL grid edge.

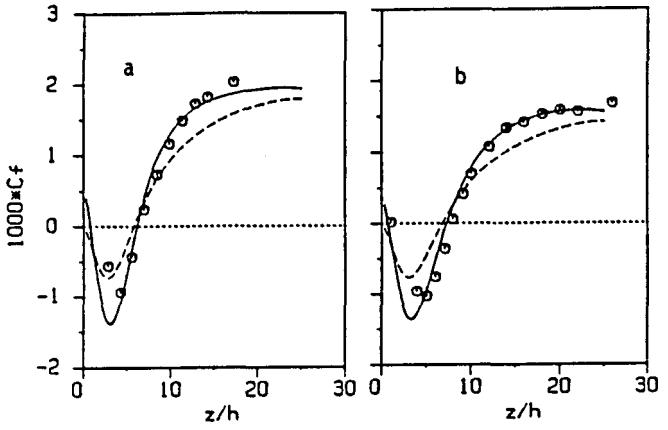

Figure 2. Skin friction for the channel flow cases of Adams (a) and Westphal (b). Solid line - BL model; Dashed line - wall functions; Symbols - data.

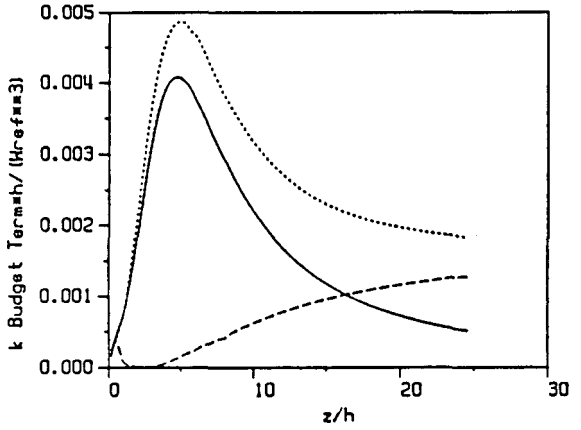

Figure 3. BL model turbulence energy budget at y^+=50 for the Adams channel flow case. Solid line - diffusion; Short dashed line - dissipation; Long dashed line - production.

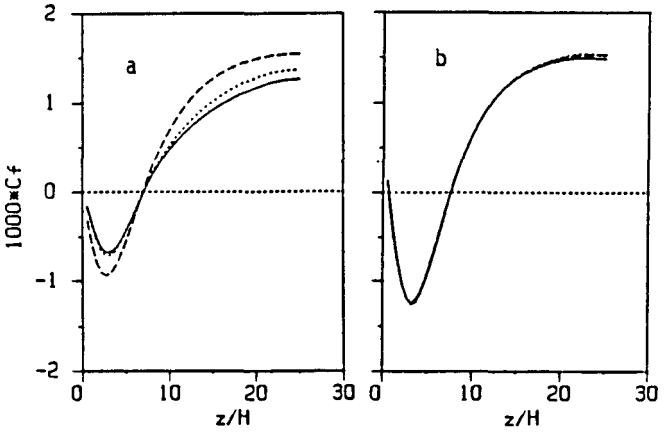

Figure 4. Skin friction for the Westphal channel flow case using grids with different near wall node positions (y_{nw}/h). (a) Wall functions; (b) BL model; Solid line - y_{nw}/h=0.05; Short dashed line - y_{nw}/h=0.025; Long dashed line - y_{nw}/h=0.01. Grid resolution was 20 x 30 for each case.

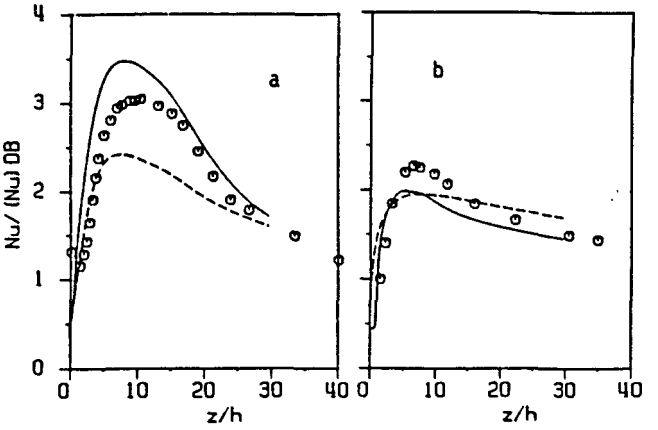

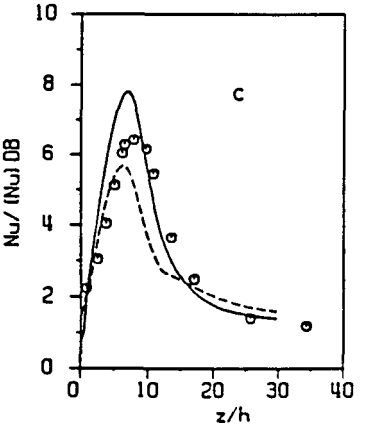

Figure 5.Nusselt number for three pipe flow cases. (a), (b), (c) - Cases 1, 2 and 3 of Table III; Solid line - BL model; Dashed line - wall functions; Symbols - data.

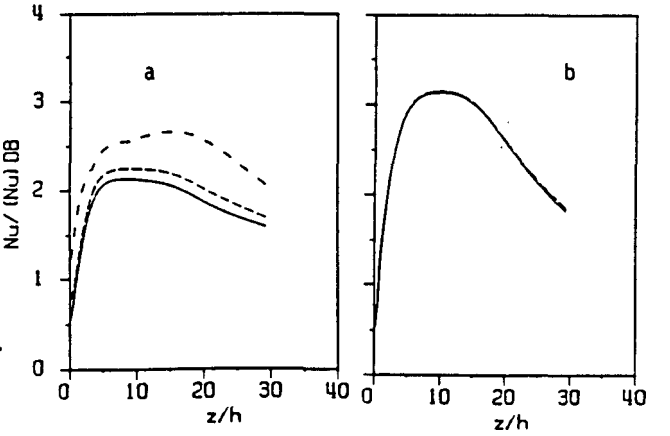

Figure 6.Nusselt number for the case 1 pipe flow of Table III using grids with different near wall node positions (y_{nw}/h). (a) Wall functions, (b) BL model; Solid line - y_{nw}/h=0.036; Short dashed line - y_{nw}/h=0.022; Long dashed line - y_{nw}/h=0.008. Grid resolution for each case was 28 x 53.

DISCLAIMER